

## High-performance GaInAs / GaAs quantum-dot lasers based on a single active layer.

F.Schäfer,<sup>a)</sup> J.P.Reithmaier, and A. Forchel

*Technische Physik, Universität Würzburg, Am Hubland, D-97074*

*Würzburg, Germany*

(Received 29 September 1998; accepted for publication 17 March 1999)

GaInAs/GaAs quantum-dot lasers were fabricated by self-organized growth in a molecular beam epitaxy system. By using a single active layer, lasers with low-threshold current densities ( $J_{th} = 144 \text{ A/cm}^2$  for a 2 mm long device) and high internal quantum efficiencies ( $>90\%$ ) were obtained. Ground-state lasing of the quantum dots was observed up to a device temperature of  $214^\circ \text{ C}$ .

©1999 American Institute of Physics. [S0003-6951(99)04720-8]

The use of quantum dots in the active layer of a semiconductor injection laser is expected to lead to improved laser properties like low-threshold current density and reduced temperature sensitivity due to the delta function-like density of states of the dots.<sup>1,2</sup> Self-assembled growth is the most promising technology to obtain quantum dots at high densities with high crystal quality.<sup>3</sup> Laser operation of self-organized (Ga, In) As/GaAs quantum dots at room temperature has already been demonstrated by several groups.<sup>4-9</sup> In order to improve the quantum efficiency, recent work on quantum-dot lasers has focused on active regions based on several layers of coupled dots. In these structures dot lasing has been demonstrated at temperatures up to  $360 \text{ K}$  ( $87^\circ \text{ C}$ ).<sup>10,11</sup>

In this letter we present results of high-performance GaInAs/GaAs quantum-dot lasers based on a single active layer. The active region is formed by  $\text{Ga}_{0.4}\text{In}_{0.6}\text{As}$ /GaAs self-organized quantum dots and is embedded in an  $\text{Al}_{0.33}\text{Ga}_{0.67}\text{As}$ /GaAs graded index separate confined hetero-structure (GRINSCH) based on a short period superlattice. The use of a superlattice structure in combination with a GRINSCH waveguide results in high internal quantum efficiencies and low-threshold current densities at room temperature.<sup>12</sup> The laser emits on the dot ground state up to a device temperature of  $214^\circ \text{ C}$  with 7 mW output power per facet. To the best of our knowledge, this is the highest operating temperature reported to date for (Ga, In) As /GaAs quantum-dot lasers. Due to the use of quantum dots as the active material, the temperature dependence of the laser emission wavelength is significantly reduced compared to GaInAs lasers based on quantum wells.

The laser samples were grown on (100)-Si:GaAs ( $n=2 \times 10^{18} \text{ cm}^{-3}$ ) substrates in an **EIKO molecular beam epitaxy system**. The structures consist of a  $1.6 \mu\text{m}$  thick  $n$ - $\text{Al}_{0.4}\text{Ga}_{0.6}\text{As}$  bottom cladding layer, a  $220 \text{ nm}$  GaAs graded index waveguide layer with a single layer of quantum dots at the center, a  $1.5 \mu\text{m}$   $\text{Al}_{0.4}\text{Ga}_{0.6}\text{As}$  upper cladding layer, and a  $100 \text{ nm}$   $p^+$ -GaAs contact layer. The graded index region was formed by a short period superlattice (SSL) with varying average Al concentration (0.30-0.15).<sup>12</sup> The SSL consists of layers of  $\text{Al}_{0.33}\text{Ga}_{0.67}\text{As}$  with a fixed width of  $2 \text{ nm}$  and GaAs with varying width ( $0.2$ - $2.4 \text{ nm}$ ). The quantum dots were grown after  $3 \text{ nm}$  GaAs with seven periods of  $0.095 \text{ nm}$   $\text{Ga}_{0.82}\text{In}_{0.18}\text{As}$  and  $0.1 \text{ nm}$  InAs to a total thickness of  $1.4 \text{ nm}$  ( $4.8 \text{ ML}$ ) covered by  $3 \text{ nm}$  GaAs. The average In concentration equals  $0.60$ . The cladding layers of the No.1 lasers were grown at  $700^\circ \text{ C}$ , the SSL at  $590^\circ \text{ C}$ , and the quantum-dot region at  $470^\circ \text{ C}$  with growth interruptions between each section. For the No.2 lasers, the substrate temperature of the upper

cladding layer was reduced to 590° C. The optical properties of quantum dots grown at temperatures used for the No.2 lasers are described elsewhere.<sup>13</sup> From both structures broad - area lasers with 50-100 μm wide stripes were fabricated. The facets of the processed lasers were cleaved to cavity lengths between 600 and 2000 μm and not coated.

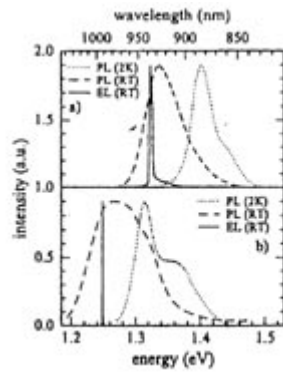


Fig.1. Photoluminescence spectra of quantum-dot Laser structure with high-[No.1,(a)] and low-[No.2,(b)] Temperature-grown upper cladding layers measured at  $T=2\text{K}$  (dotted line) and room temperature (dashed line) in comparison to room-temperature laser spectra at  $J=1.5 \times J_{th}$  (solid line)

Appl. Phys. Lett., Vol. 74, No. 20, 17 May 1999

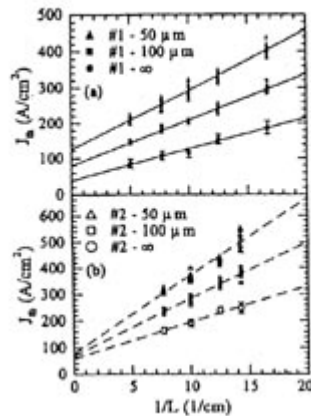


Fig.2. Dependence of the threshold current density on the cavity length for No.1(a) and No.2(b) lasers. Values are shown for stripe widths of 50μm (▲/△) And 100μm (■/□) and extrapolated to infinite width (○/●).

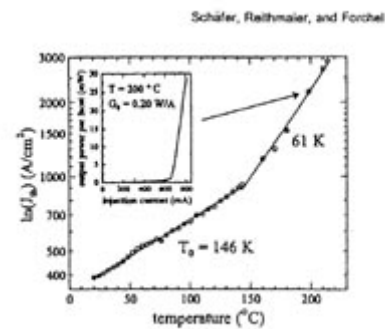


Fig.3. Threshold current density of a 600μm × 50μm broad-area No.1 laser different temperature ranging from 20 up to 214° C. The inset shows a light output curve at 200° C.

The lasers have been characterized at different temperatures ranging from 20 up to 215° C. Figure 1 (a) shows a photoluminescence (PL) spectrum of laser structure No.1 measured at  $T=2\text{K}$  using a  $\text{Kr}^+$  laser for excitation (dotted line). The spectrum includes two emission bands which can be fitted with very good agreement by two Gaussian functions centered at 1.402 and 1.442 eV, with full width at half maxima (FWHM) of 36 and 41 meV, respectively. The PL peak at an energy of 1.402 eV corresponds to the ground-state transitions, the second peak at 1.442 eV to the first excited states of the quantum dots. For the No.2 lasers [Fig.1(b)], we observe a similar two-feature structure centered at 1.312 and 1.354 eV. The difference in the transition energies for the Nos. 1 and 2 lasers is caused by In diffusion<sup>14</sup> during the high-temperature growth process of the upper cladding layer in the No. 1 lasers, which reduces the potential depth of the quantum dots. If we compare the PL at room temperature (dashed line) to the laser spectrum (solid line) at an injection current of  $J=1.5 \times J_{th}$  (see Fig.1), it can be seen that both quantum-dot laser structures show lasing operation on the low-energy side of the peak, as expected for ground-state emission.

At room temperature the internal quantum efficiency is 95% and 91% for the Nos. 1 and 2 lasers, respectively. Figure 2 shows the measured dependence of the threshold current density on the cavity length for a stripe width of 50 and 100  $\mu\text{m}$  and extrapolated to infinite width<sup>15</sup> for the No.1 [Fig.2(a)] and the No.2 [Fig.2(b)] lasers. The No.2 lasers show slightly increased threshold current densities, which we attribute to the higher internal absorption caused by the reduced material quality due to the low-temperature growth. A broad-area threshold current density as low as 144  $\text{A}/\text{cm}^2$  is achieved ( $L=2\text{mm}$ , stripe width 100 $\mu\text{m}$ , No.1 lasers). By extrapolating the data to infinite length and width a lower limit for the threshold current density of about 40  $\text{A}/\text{cm}^2$  (No.1) and 60  $\text{A}/\text{cm}^2$  (No.2) is estimated.

For temperature-dependent measurements pulsed operation was used (300 ns pulses with 1 ms duty cycle) to avoid additional heating by current injection. Figure 3 shows the temperature dependence of the threshold current density of a 600 $\mu\text{m} \times 50\mu\text{m}$  broad area No.1 laser. The inset of Fig.3 shows a light output curve at an operation temperature of 200° C. The efficiency is still high and achieves values of  $G_0=0.20 \text{ W}/\text{A}$  per facet. An output power of more than 25mW could be measured. A maximum operation temperature of 214° C was obtained with an output power of 7mW per facet from an uncoated device. The maximum output power for devices measured above 200° C is mainly limited by injection current restrictions. The external quantum efficiency decreases from 48% at room temperature to 14% at 214° C. Type No.2 lasers behave similarly. On such devices a maximum operation temperature of 173° C was achieved.

Within a certain temperature range the threshold current density  $J_{\text{th}}$  can be described by an exponential temperature dependence<sup>16</sup>

$$J_{\text{th}}=J_0 \times \exp(T/T_0), \quad (1)$$

with the characteristic temperature  $T_0$ . Although the parameters  $J_0$  and  $T_0$  are temperature dependent, they can be approximated by constant values for certain temperature ranges. As shown by the data in the temperature range between 20 and 143° C in Fig.3, a fit to the temperature dependence of the threshold provides a  $T_0$  value of 146K. For ideal quantum-dot lasers a negligible temperature dependence is expected, because the energy distribution of the carriers is fixed by the discrete energy levels of the quantum dots. However, this is only valid coupling between the dots via continuous states above the quantum-dot barriers can be neglected. In real quantum-dot structures the finite barrier height has to be taken into account. Therefore, the achieved characteristic temperatures do not exceed the  $T_0$  values of quantum-well lasers (e.g., > 300 K up to 75° C).<sup>12</sup> Additionally, the inclusion of a wetting layer in the structures reduces the potential barrier with respect to the GeAs band edge. Therefore, we attribute the observed  $T_0$  value of 146 K at room temperature mainly to the influence of the wetting layer, which should exist even if it cannot be detected in PL spectra. As a consequence, the  $T_0$  value is constant up to 143° C operation temperature and a threshold current density of 452  $\text{A}/\text{cm}^2$  at 145° C (1.3  $\times$  0.1mm<sup>2</sup> broad-area laser) could be achieved. Above 143° C,  $T_0$  is reduced to a value of 61 K, most likely due to thermionic emission from the dots into the waveguide.

In Fig.4 the wavelength shift of the quantum-dot lasers is plotted as a function of the operation temperature. No kinks are observed, which would be expected if the lasing operation would switch to transitions of higher quantum-dot states. The wavelength increases nearly linearly with a slope of 0.19 nm/K (No.1) and 0.17 nm/K (No.2), which corresponds to a decrease of the emission energy of -0.26 meV/K (No.1) and -0.21 meV/K (No.2), respectively. This value agrees well with

the wavelength shift published by other groups for lasing on the quantum-dot ground-state, e.g., 0.22 nm/K.<sup>10</sup> The kinkless and weak temperature dependence of the emission wavelength indicates that the laser operates on the ground state over the whole temperature range from 20 up to 214° C. For comparison reasons the wavelength shift of a quantum-well-based laser<sup>12</sup> is also plotted with a typical value of 0.33 nm/K. This is about 80% higher than that of quantum-dot lasers.

Appl. Phys. Lett., Vol. 74, No. 20, 17 May 1999

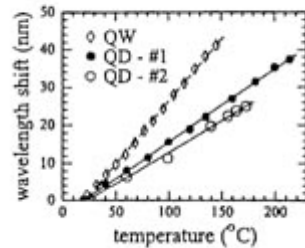


Fig.4. Emission wavelength shift of a quantum-well laser ( $\diamond$ ), No1 ( $\bullet$ ) and No.2 quantum-dot laser ( $\circ$ ).

In summary, we have presented data on GaInAs/GaAs single-layer quantum-dot lasers grown by molecular beam epitaxy. We achieved lasing on the dot ground state up to an operating temperature of 214° C. Low-threshold current densities of 144 A/cm<sup>2</sup> and internal quantum efficiencies of more than 90% could be measured. In comparison to quantum-well lasers, a reduced temperature dependence of the emission wavelength was observed which makes quantum-dot lasers more suitable for uncooled device applications.

The authors would like to thank A. Wolf for expert technical assistance for device processing and F. Klopff for experimental assistance. The financial support by the State of Bavaria and the European Community (ESPRIT) is gratefully acknowledged.

- 1 Y.Arakawa and H. Sakaki, Appl. Phys. Lett. 40, 939 (1982).
- 2 M.Asada, Y.Miyamoto, and Y.Suematsu, IEEE J.Quantum Electron. QE-22, 1915(1986).
- 3 D.Leonard, M.Krishnamurthy, C.M.Reaves,S.P.Denbaars, and P.M.Petroff, Appl. Phys. Lett. 63, 3203 (1993).
- 4 F. Heinrichsdorff, M.- H.Mao, N. Kirstaedter, A. Krost, D. Bimberg, A. O. Kosogov, and P. Werner, Appl. Phys. Lett. 71,22 (1997).
- 5 M.V. Maximov, Yu. M. Shernyakov, A F.Tsatsul'nikov, A.V.Lunev, A.V.Sakharov, V.M.Ustinov, A.Yu.Egorov, A.E.Zhukov, A.R.Kovsh, P.S.Kop'ev, L.V.Asryan, Zh. I.Alferov, N.N.Ledentsov, D.Bimberg, A.O.Kosogov, and P.Werner, J.Appl.Phys. 83,5561 (1998).
- 6 K. Kamath, P.Bhattacharya, T.Sosnowski, T.Norris, and J.Phillips, Electron. Lett. 32, 1374 (1996)
- 7 R.Mirin, A.Gossard, and J.Bowers, Electron. Lett. 32, 1732 (1996).
- 8 H.Shoji, Y.Nakata, K.Mukai, Y.Sugiyama, M.Sugawara, N.Yokoyama, and H.Ishikawa, Electron. Lett. 32, 2023 (1996).
- 9 D.L.Huffaker, G Park, Z.Zou, O.B.Shchekin, and D.G.Deppe, Appl. Phys. Lett. 73, 2564 (1998)
- 10 V.M.Ustinov, A.Yu.Eigorov, A.R.Kovsh, A.E.Zhukov, M.V.Maximov, A.F.Tsatsul'nikov, N.Yu.Gordeev,S.V.Zaitsev, Yu.M.Shemyakov, N.A Bert, P.S.Kop'ev, Zh.I.Alferov, N.N.Ledentsov, J.Bohrer, D.Bimberg, A.O.Kosogov, P.Werner, and U.Gosele, J Cryst. Growth 175/176, 689 (1997).
- 11 M.V.Maximov, I.V.Kochnev, Y.M.Shernyakov, S.V. Zaitsev, N.Yu.Gordeev, A F.Tsatsul'nikov, A.V.Sakharov, I.L.Krestnikov, P.S.Kop'ev, Zh.I.Alferov, N.N Ledentsov, D. Bimberg, A O. Kosogov, P, Werner, and U.Gosele, Jpn. J. Appl. Phys., Part 1 36, 4221 (1997).
- 12 F.Schafer, B.Mayer, J.P.Reithmaier and A.Forchel, Appl.Phys. Lett. 73, 2863 (1998).
- 13 A.Kuther, M.Bayer, A.Forchel, A.Gorbunov, V. B Tirnofeev, F. Schafer, and J. P. Reithmaier, Phys. Rev. B 58, R7508 (1998).

- 14 R.Leon, Y.Kim, C.Jagadish, M.Gal, J.You, and D.J.H.Cockayne, Appl. Phys. Lett. 69, 1888 (1996).
- 15 N.Chand, E.E.Becker, J.P.van der Ziel, S.N.G.Chu, and N.K.Dutta, Appl. Phys.Lett. 58, 1704 (1991).
- 16 L.A.Coldren and S.W.Corzine, Diode Lasers and Photonic Integrated Circuits (Wiley, New York 1995).